UNIVERSIDADE DE SÃO PAULO

INSTITUTO DE FÍSICA
CAIXA POSTAL 66318
05389-970 SÃO PAULO - SP
BRASIL

PUBLICAÇÕES

IFUSP/P-1175

THE SU (3) LIPKIN MODEL. (I): THE THERMODYNAMICS

M.O. Terra
Instituto de Física, Universidade de São Paulo

A.H. Blin, B. Hiller, C. Providência and J. da Providência
Centro de Física Teórica (INIC), Universidade de Coimbra,
P-3000 Coimbra, Portugal

M.C. Nemes
Departamento de Física, Instituto de Ciências Exatas,
Universidade Federal de Minas Gerais,
C.P. 702,31270 Belo Horizonte, MG, Brazil

Setembro/1995

The SU(3) Lipkin model. (I): The thermodynamics

M.O.Terra[1], A.H.Blin[2], B.Hiller[2], M.C.Nemes[3], C.Providência[2] and J. da Providência[2]

[1] *Instituto de Física, Departamento de Física-Matemática, Universidade de São Paulo, C.P. 66318, São Paulo, SP, Brazil.*

[2] *Centro de Física Teórica (INIC), Universidade de Coimbra, P-3000 Coimbra, Portugal.*

[3] *Departamento de Física, Instituto de Ciências Exatas, Universidade Federal de Minas Gerais, C.P. 702, 31270 Belo Horizonte, MG, Brazil.*

Abstract

We present a detailed analysis of the thermodynamical properties of the SU(3) Lipkin model. Two phase transitions are found which depend on the interplay between temperature and coupling strength. The three thermodynamic phases are characterized by a specific behavior of the levels populations. The adequacy of the approximation, which allows for analytic results, is tested numerically.

PACs Number: 0545, 0520, 2160F

I. INTRODUCTION

Soluble models have always played a decisive role in unveiling the essential physics of various systems. In particular, we quote the class of Curie Weiss systems [1], i.e., systems for which the mean field approximation becomes exact as the number of particles tends to infinity. In the context of quantum optics, the Maser model [2] is well known for predicting the superradiant transition and other relevant thermodynamical properties. The Pairing model [3] which illustrates properties of superconductivity and finally in the context of nuclear physics we have the well known Lipkin model [4, 5]. It has originally been conceived as a toy model to test the validity of various many body techniques. Recently the thermodynamical properties of the model in its integrable SU(2) version has been studied [6]. It has been found that the model predicts two phases (one phase transition) and that, qualitatively speaking, temperature effects tend to counterbalance the effects of the two body interaction. The mathematical structure of the SU(3) version of the model is far richer. In particular, it is nonintegrable and its classical limit has been shown to exhibit chaotic behavior [5]. To our knowledge its thermodynamical properties have never been investigated.

It is the purpose of the present contribution to give a detailed account of the relevant thermodynamical properties of the SU(3) Lipkin model. We find that in this case there are two phase transitions and correspondingly three different regimes which we call: *weak coupling, intermediate coupling and strong coupling regimes.* These

regimes are characterized by given intervals of coupling strength and temperature. For finite N (number of particles) we are able to show that in the strong coupling regime the symmetric representation of the SU(3) group is the dominant one and therefore responsible for all thermodynamical properties. For the other regimes the relative contribution of other representations become nonnegligible. All the results are given essentially in analytic form.

In section II we present the model and in section III the thermodynamical properties are derived in the mean field approximation. Section IV is devoted to the study of the adequacy of the mean field approximation by comparison with finite N results. Finally section V contains conclusions.

II. THE SU(3) LIPKIN MODEL

The model [5] represents a system of N interacting fermions which can occupy three N-fold degenerate shells. Its Hamiltonian is given by

$$H = \sum_{i=0}^{2} \epsilon_i G_{ii} + \frac{1}{2} V \sum_{i \neq j=0}^{2} G_{ij}^2, \tag{1}$$

where the G_{ij} are generators of an $U(3)$ algebra, which obey the commutation relation

$$[G_{ij}, G_{kl}] = \delta_{jk} G_{il} - \delta_{il} G_{kj}. \tag{2}$$

In terms of fermionic creation and annihilation operators, they can be written as

$$G_{ij} = \sum_{m=1}^{N} a_{im}^{\dagger} a_{jm}, \qquad G_{ij}^{\dagger} = G_{ji}, \qquad i,j = 0,1,2. \tag{3}$$

An additional constraint is imposed by particle number conservation, i.e., $G_{00} + G_{11} + G_{22} = N$. Therefore the dynamical symmetry corresponds to that of an $SU(3)$ algebra. The energies of the shells are chosen to be symmetrical about zero, i.e., $\epsilon_2 = -\epsilon_0 = \epsilon$ and $\epsilon_1 = 0$. In the present work all the energies are given in units of $N\epsilon$. The scaled coupling constant is defined as $\chi = \frac{(N-1)V}{\epsilon}$, as usual.

The coupling term of this Hamiltonian is chosen so that there is no interaction between particles in the same level. It promotes the scattering of particles between any two of the levels.

III. THERMODYNAMICS

In this section we shall derive the thermodynamical properties of the model from an equilibrium state which is constructed within the scheme of a variational mean field [7]. In the large N limit, the mean field approximation becomes exact and the calculation of the relevant thermodynamical quantities becomes simpler. This has been done for the case of the integrable $SU(2)$ Lipkin model with particular emphasis on the phase transition behavior [6]. In the present case the calculations are much more involved. We find various mathematical solutions which extremize the free energy, only three of them corresponding to physical situation in different temperature intervals.

A. Equilibrium States

We start by constructing the variational mean field density matrix as follows,

$$D_0 = Kexp(-\beta h_{MF}), \tag{4}$$

where

$$\begin{aligned} h_{MF} &= \alpha_1(G_{11}-G_{00}) + \alpha_2 G_{01} + \alpha_2^* G_{10} + \alpha_3(G_{22}-G_{00}) + \\ &+\alpha_4 G_{02} + \alpha_4^* G_{20} + \alpha_5(G_{11}-G_{22}) + \alpha_6 G_{12} + \alpha_6^* G_{21} \end{aligned} \tag{5}$$

and K is a normalization factor. The set of variational parameters α_i's are obtained by minimizing the free energy

$$\beta F = \beta Tr(D_0 H) + Tr(D_0 \ln D_0), \tag{6}.$$

where β is $1/(k_B T)$, k_B the Boltzmann constant and T the temperature. For technical reasons it is convenient to go to the diagonal representation of D_0.

$$D = U D_0 U^\dagger = \frac{1}{Z} e^{\beta_1(G_{11}-G_{00})} e^{\beta_2(G_{22}-G_{00})}, \tag{7}$$

where

$$Z = z^N = Tr(e^{\beta_1(G_{11}-G_{00})} e^{\beta_2(G_{22}-G_{00})}), \tag{8}$$

$$U = U_3 U_2 U_1 = e^{is_3} e^{is_2} e^{is_1}, \tag{9}$$

with

$$s_1 = z_1 G_{10} + z_1^* G_{01}, \qquad s_2 = z_2 G_{20} + z_2^* G_{02}, \qquad s_3 = z_3 G_{21} + z_3^* G_{12}. \tag{10}$$

The free energy becomes

$$\beta F = \beta Tr(DUHU^\dagger) + Tr(D \ln D). \tag{11}$$

The variational parameters are $\theta_1 = iz_1$, $\theta_2 = iz_2$, $\theta_3 = iz_3$, β_1 and β_2. It is easy to check from the expression for the free energy that the real part of z_1, z_2 and z_3 are irrelevant for the stationary properties in the case $\chi < 0$.

The free energy scaled by N can then be written as

$$\begin{aligned} \bar{F} = \frac{F}{N} &= -\cos(2\theta_2)(T_2 - \sin^2\theta_3 T_3) + \frac{1}{2}\sin(2\theta_1)\sin\theta_2\sin(2\theta_3)T_3 + \\ &+\sin^2\theta_1\left(T_1 + \sin^2\theta_3 T_3 - \sin^2\theta_2(T_2 - \sin^2\theta_3 T_3)\right) + \\ &+\frac{\chi}{4}\left\{\cos^2\theta_2\sin^2(2\theta_3)T_3^2 + \sin^2(2\theta_2)(T_2 - \sin^2\theta_3 T_3)^2 + \right. \\ &+\{\sin(2\theta_1)(T_1 - \sin^2\theta_2 T_2) + T_3[\sin(2\theta_1)(1+\sin^2\theta_2)\sin^2\theta_3 + \\ &\left.+\cos(2\theta_1)\sin\theta_2\sin(2\theta_3)]\}^2\right\} - \frac{1}{\beta}(\beta_1 T_1 + \beta_2 T_2 + \ln z), \end{aligned} \tag{12}$$

where

$$T_1 = \frac{Tr(D(G_{00}-G_{11}))}{N} = \frac{e^{-(\beta_1+\beta_2)} - e^{\beta_1}}{z}, \tag{13}$$

$$T_2 = \frac{Tr(D(G_{00} - G_{22}))}{N} = \frac{e^{-(\beta_1+\beta_2)} - e^{\beta_2}}{z}, \tag{14}$$

$$T_3 = \frac{Tr(D(G_{11} - G_{22}))}{N} = T_2 - T_1, \tag{15}$$

$$z = e^{\beta_1} + e^{\beta_2} + e^{-(\beta_1+\beta_2)}. \tag{16}$$

Minimizing eq. (12) with respect to these parameters, setting

$$\begin{aligned}
\frac{\partial \bar{F}}{\partial \theta_1} &= \cos(2\theta_1)\sin\theta_2\sin(2\theta_3)T_3 + \sin(2\theta_1)\left(T_1 + \sin^2\theta_3 T_3 - \sin^2\theta_2(T_2 - \sin^2\theta_3 T_3)\right) + \\
&+ \chi\Big\{\{\sin(2\theta_1)(T_1 - \sin^2\theta_2 T_2) + T_3[\sin(2\theta_1)(1+\sin^2\theta_2)\sin^2\theta_3 + \cos(2\theta_1)\sin\theta_2\sin(2\theta_3)]\} \\
&\quad \{\cos(2\theta_1)(T_1 - \sin^2\theta_2 T_2) + T_3[\cos(2\theta_1)(1+\sin^2\theta_2)\sin^2\theta_3 - \sin(2\theta_1)\sin\theta_2\sin(2\theta_3)]\}\Big\} \\
&= 0,
\end{aligned} \tag{17}$$

$$\begin{aligned}
\frac{\partial \bar{F}}{\partial \theta_2} &= 2\sin(2\theta_2)(T_2 - \sin^2\theta_3 T_3) + \sin(2\theta_1)\cos\theta_2\sin(2\theta_3)\frac{T_3}{2} - \sin^2\theta_1\sin(2\theta_2)(T_2 - \sin^2\theta_3 T_3) + \\
&+ \frac{\chi}{4}\Big\{-\sin(2\theta_2)\sin^2(2\theta_3)\,T_3^2 + 2\sin(4\theta_2)(T_2 - \sin^2\theta_3 T_3)^2 + \\
&\quad +2\{\sin(2\theta_1)(T_1 - \sin^2\theta_2 T_2) + T_3[\sin(2\theta_1)(1+\sin^2\theta_2)\sin^2\theta_3 + \cos(2\theta_1)\sin\theta_2\sin(2\theta_3)]\} \\
&\quad \{-\sin(2\theta_1)\sin(2\theta_2)T_2 + T_3[\sin(2\theta_1)\sin(2\theta_2)\sin^2\theta_3 + \cos(2\theta_1)\cos\theta_2\sin(2\theta_3)]\}\Big\} \\
&= 0,
\end{aligned} \tag{18}$$

$$\begin{aligned}
\frac{\partial \bar{F}}{\partial \theta_3} &= \cos(2\theta_2)\sin(2\theta_3)T_3 + \sin(2\theta_1)\sin\theta_2\cos(2\theta_3)T_3 + \sin^2\theta_1\sin(2\theta_3)T_3(1+\sin^2\theta_2) + \\
&+ \frac{\chi}{2}T_3\Big\{\cos^2\theta_2\sin(4\theta_3)\,T_3 - \sin^2(2\theta_2)\sin(2\theta_3)(T_2 - \sin^2\theta_3 T_3) + \\
&\quad +\{\sin(2\theta_1)(T_1 - \sin^2\theta_2 T_2) + T_3[\sin(2\theta_1)(1+\sin^2\theta_2)\sin^2\theta_3 + \cos(2\theta_1)\sin\theta_2\sin(2\theta_3) \\
&\quad \{\sin(2\theta_1)(1+\sin^2\theta_2)\sin(2\theta_3) + 2\cos(2\theta_1)\sin\theta_2\cos(2\theta_3)\}\} \\
&= 0,
\end{aligned} \tag{19}$$

$$\begin{aligned}
\frac{\partial \bar{F}}{\partial \beta_j} &= -[\cos(2\theta_2) + \sin^2\theta_1\sin^2\theta_2]A_{j2} + \sin^2\theta_1 A_{1j} + (A_{j2} - A_{1j}) \\
&\quad \{\cos(2\theta_2)\sin^2\theta_3 + \frac{1}{2}\sin(2\theta_1)\sin\theta_2\sin(2\theta_3) + \sin^2\theta_1\sin^2\theta_3(1+\sin^2\theta_2)\} \\
&+ \frac{\chi}{2}\Big\{(A_{j2} - A_{1j})\cos^2\theta_2\sin^2(2\theta_3)T_3 + \sin^2(2\theta_2)(T_2 - \sin^2\theta_3 T_3)[A_{j2} - (A_{j2} - A_{1j})\sin^2\theta \\
&\quad +\{\sin(2\theta_1)(T_1 - \sin^2\theta_2 T_2) + T_3[\sin(2\theta_1)(1+\sin^2\theta_2)\sin^2\theta_3 + \cos(2\theta_1)\sin\theta_2\sin(2\theta_3) \\
&\quad \{\sin(2\theta_1)(A_{1j} - A_{j2}\sin^2\theta_2) + (A_{j2} - A_{1j})[\sin(2\theta_1)(1+\sin^2\theta_2)\sin^2\theta_3 + \\
&\quad + \cos(2\theta_1)\sin\theta_2\sin(2\theta_3)]\}\Big\} - \frac{1}{\beta}(T_j + \beta_1 A_{1j} + \beta_2 A_{j2} + \frac{\partial}{\partial\beta_j}\ln z) = 0, \qquad j = 1,2
\end{aligned} \tag{20}$$

where

$$A_{11} = \frac{\partial T_1}{\partial \beta_1} = -\frac{1}{z^2}\left(e^{-\beta_1} + 4e^{-\beta_2} + e^{(\beta_1+\beta_2)}\right), \tag{21}$$

$$A_{22} = \frac{\partial T_2}{\partial \beta_2} = -\frac{1}{z^2}\left(e^{-\beta_2} + 4e^{-\beta_1} + e^{(\beta_1+\beta_2)}\right), \tag{22}$$

$$A_{12} = A_{21} = \frac{\partial T_1}{\partial \beta_2} = \frac{\partial T_2}{\partial \beta_1} = -\frac{1}{z^2}\left(2e^{-\beta_1} + 2e^{-\beta_2} - e^{(\beta_1+\beta_2)}\right), \qquad (23)$$

$$\frac{\partial}{\partial \beta_j} \ln z = \frac{1}{z}\left(e^{\beta_j} - e^{-(\beta_1+\beta_2)}\right), \qquad j = 1,2. \qquad (24)$$

We find numerically that the extremum condition can be obtained for $\theta_3 = 0$ or π. Substituting this results in the above equations we obtain analytical expressions for candidates of solutions θ_1 and θ_2 in various χ and temperature ranges. These results are shown in Table I. The solutions found in this table are substituted in eqs.(20) in order to find β_1 and β_2 numerically. We find that the solutions which correspond to a minimum are three (1,9 and 11 in Table I), each one of them valid in a different temperature and coupling strength interval. We describe them in detail next.

Strong Coupling Regime (SCR): Valid for $\chi T_1 \leq -3$. It implies that $\chi \leq -3$ and $\beta \geq \beta_{cr1}$ (β_{cr1} is found numerically and displayed in the figures).

The parameters in this case are

$$\beta_1 = \beta_2 \quad \Rightarrow \quad T_1 = T_2 = T,$$

$$\cos(2\theta_1) = \frac{3}{3-2\chi T}, \qquad \sin^2\theta_2 = \frac{3+\chi T}{3\chi T}, \qquad \theta_3 = 0.$$

Intermediate Coupling Regime (ICR): Valid for $\chi \leq -1$ and temperature interval that has to be found numerically

$$\beta_{cr2} \leq \beta \leq \beta_{cr1} \qquad \text{for} \qquad \chi \leq -3$$

$$\beta \geq \beta_{cr2} \qquad \text{for} \qquad -3 \leq \chi \leq -1$$

or in more compact form

$$-3 \leq \chi T_1 \leq -1.$$

And the parameters

$$\cos(2\theta_1) = -\frac{1}{\chi T_1}, \qquad \theta_2 = 0, \qquad \theta_3 = 0.$$

Weak Coupling Regime (WCR): Valid for all values of χ being a minimum when

$$\beta \leq \beta_{cr2} \qquad \text{for} \qquad \chi \leq -1$$

and

$$\text{any } \beta \qquad \text{for} \qquad \chi > -1$$

or in more compact form

$$\chi T_1 \leq -1.$$

And the parameters

$$\theta_1 = \theta_2 = \theta_3 = 0, \qquad \beta_1 = 0, \qquad \beta_2 = -\beta.$$

The free energy corresponding to these solutions are shown in Figs. 1(a),(b) and (c). In the first case (Fig. 1(a)) we show, as a function of inverse temperature a

particular χ value, $\chi = -6.0$ for which the three solutions are present. Note that one has two phase transitions, the first one from SCR solution to ICR solution at $\beta_{cr1} = 0.4621$ and the second from ICR solution to WCR solution at $\beta_{cr2} = 0.4258$. In Fig. 1(b) which corresponds to a lower χ value one finds only one phase transition from ICR solution to WCR solution. In this case SCR solution does not exist. Figure 1(c) does not present any phase transition, WCR solution is the only one. Thus, we conclude that increasing the temperature effectively "weakens" the coupling. In the SCR the coupling is "active" in all shells in the sense that neither θ_1 nor θ_2 are zero. In the ICR the solution is identical to the one obtained in the $SU(2)$ case for the deformed case [6]. The WCR is always a mathematical solution and becomes the physical solution for sufficiently high temperature values or weak enough coupling strengths. In this case χ does not play any role.

Another instructive quantity is the average population difference of the levels as a function of χ and β, namely

$$P_{01} = \frac{\langle T_1 \rangle}{N} = \frac{Tr(DU(G_{00} - G_{11})U^\dagger)}{N} = \cos(2\theta_1)(T_1 + \sin^2\theta_3 T_3 + - \sin^2\theta_2(T_2 - \sin^2\theta_3 T_3)) + \sin(2\theta_1)\sin\theta_2\sin(2\theta_3)T_3, \quad (25)$$

$$P_{02} = \frac{\langle T_2 \rangle}{N} = \frac{Tr(DU(G_{00} - G_{22})U^\dagger)}{N} = \cos(2\theta_2)(T_2 - \sin^2\theta_3 T_3) + -\frac{1}{2}\sin(2\theta_1)\sin\theta_2\sin(2\theta_3)T_3 - \sin^2\theta_1(T_1 + \sin^2\theta_3 T_3 +$$

$$- \sin^2\theta_2(T_2 - \sin^2\theta_3 T_3)), \quad (26)$$

where $P_{01(02)}$ stands for the difference of the average population of the first (second) excited level and the ground level.

They are shown in Figs. 2 (a) and (b). For the strong coupling regime both population differences are held constant up to $\beta = \beta_{cr1}$. This is certainly due to the fact that the coupling term is important. For $\beta_{cr2} \leq \beta \leq \beta_{cr1}$ one sees the increase of temperature effectively diminishes the role played by the interaction. In this case the difference of population between levels 0 and 2 diminishes whereas the behavior of difference of populations between levels 0 and 1 remains the same. Below β_{cr2} the coupling strength is no longer important, and as expected, the system will tend to populate all levels equally as required by maximizing the entropy.

The entropy and internal energy are shown in Fig. 3. For low temperature the entropy is very small and the free energy will be dominated by the contribution of the internal energy. As the temperature is increased these roles are inverted, as expected.

The two second order phase transitions are clearly reflected in the specific heat of the system, shown in Fig. 4. The behavior of the order parameters of the model is shown in Fig. 5. The average values of the operators G_{02} (or G_{20}) and G_{01} (or G_{10}) can be chosen as order parameters of the first ($SCR \rightarrow ICR$) and second ($ICR \rightarrow WCR$) phase transitions respectively. This is due to the fact that their expectation values vanish for temperature higher than the corresponding critical temperatures.

IV. FINITE N RESULTS AND THE MEAN FIELD APPROXIMATION

The mean field approximation used in the present work involves all the different irreducible representations of the SU(3) group. It is possible to investigate their role in an exact calculation for finite N. For example, in Fig. 6 we display the eingenvalues of the Hamiltonian (1) for $N = 6$ and $\chi = -6.0$. They are separated according to the irreducible representations they belong to. The 3^6 states are distributed in the various representations in the following way

$$[3]\otimes[3]\otimes[3]\otimes[3]\otimes[3]\otimes[3] = [28]\oplus 5\times[35]\oplus 9\times[27]\oplus 10\times[10]\oplus 5\times[\overline{10}]\oplus 16\times[8]\oplus 5\times[1] \tag{27}$$

where the symbols in brackets correspond to the representation illustrated in Fig. 7.

We are now in a position to calculate the relative contribution of the various irreducible representations as a function of temperature. For this purpose we define

$$P_{[a]} = \sum_{E_j\in[a]} Y_{[a]}\frac{\exp(-\beta E_j)}{Z}, \tag{28}$$

where $Y_{[a]}$ is the multiplicity factor of the representation $[a]$.

In Fig. 8 we show $P_{[a]}$ as a function of temperature. We see that for the strong coupling regime the main contribution comes from the symmetric representation. As the temperature increases the other irreducible representations start to give nonnegligible contribution.

In order to illustrate the adequacy of the m.f.a. we compare the exact result for the free energy obtained for $N = 4$ and $N = 6$ with the mean field result. The numerical calculation is very involved, therefore we have stopped at $N = 6$. However the convergence is well illustrated (see Fig. 9). For low enough temperatures when the symmetric representation alone dominates the behavior of the system it is seen that the mean field result reproduces very well the exact average free energy.

V. CONCLUDING REMARKS

We have presented a detailed investigation of the thermodynamical properties of the SU(3) Lipkin model. We show that depending on the temperature and coupling strength range the system can exhibit three regimes and two phase transitions. For finite N the strong coupling regime is shown to be dominated by the symmetric representation of the group whereas in the two other regimes other irreducible representations also play a role.

The present investigation is an essential step towards the study of bifurcation of equilibria in the thermal dynamics of the system. The full thermal dynamics can also be derived in the context of the same approximation. Investigation along these lines is presently under way.

ACKNOWLEDGEMENTS

We gratefully acknowledge many groups discussions with the colleagues K. Furuya, F.Camargo, G.Pellegrino (UNICAMP), A.F.R. de Toledo Piza and M. Trindade dos Santos (USP). This work was partially supported by JNICT, CNPq and FAPESP.

Referências

[1] L.G.Yaffe, Rev.Mod.Phys. **54**, 407 (1982).

[2] K.Hepp and E.H.Lieb, Ann.Phys. **76**, 360 (1973); A.H.Blin, B.Hiller, M.C.Nemes and J. da Providência, J.Phys. A **25**, 2243 (1992).

[3] S.J.Krieger and K.Goeke, Nucl.Phys. A **234**, 269 (1974).

[4] H.J.Lipkin, N.Meshkov and J.Glick, Nucl.Phys. **62**, 188 (1965).

[5] S.Y.Li, A.Klein and R.M.Dreizler, J.Math.Phys. **11**, 975 (1970); E.Moya de Guerra and F.Villars, Nucl.Phys. A **298**, 109 (1978); R.D.Williams and S.E.Koonin,Nucl.Phys. A **391**, 72 (1982); D.C.Meredith, S.E.Koonin and M.R.Zirnbauer, Phys.Rev. A **37**, 3499 (1988); P.Lebouf and M.Saraceno, Phys.Rev. A **41**, 4614 (1990); P.Lebouf and M.Saraceno, J.Phys. A **23** 1745 (1990); P.Lebouf, D.C.Meredith and M.Saraceno, Ann.Phys.(NY) **208**, 333 (1991).

[6] M.O.Terra, A.H.Blin, B.Hiller, M.C.Nemes, C.Providência and J. da Providência, J.Phys. A **27**, 697 (1994).

[7] J.da Providência and C.Fiolhais, Nucl.Phys. A **435**, 190 (1985); M.Yamamura, J.daProvidência and A.Kuriyama, Nucl.Phys. A **514**, 461 (1990); M.Yamamura, J.da Providência J, A.Kuriyama and C.Fiolhais, Prog.Theor.Phys. **81**, 1198(1989).

[8] M.O.Terra, A.H.Blin, B.Hiller, M.C.Nemes, C.Providência and J. da Providência,"*The SU(3) Lipkin model: (II) The thermal chaotic classical dynamics*", to be published.

FIGURE CAPTIONS

FIG. 1. The free energy $\bar{F}$ as function of inverse temperature β for three different values of coupling parameter (a) $\chi = -6.0$, (b) $\chi = -2.0$ and (c) $\chi = -0.6$. Note that in (a) there is three phases (they are separated by a vertical dotted line), in (b) two phases and in (c) just one phase. The critical inverse temperatures are indicated.

FIG. 2. P_{01} and P_{02} as function of inverse temperature β for two different values of coupling parameter (a) $\chi = -6.0$ and (b) $\chi = -2.0$.

FIG. 3. The internal energy $\bar{E}$ and the entropy $\bar{S}$ as function of inverse temperature for $\chi = -6.0$. The values of critical inverse temperature β_{cr1} and β_{cr2} at which there are phase transitions are shown and the phases are separated by a vertical dotted line.

FIG. 4. The specific heat of the system as function of inverse temperature for $\chi = -6.0$. Note the two second order phase transitions.

FIG. 5. Order parameters $< G_{02} >$ (ou $< G_{20} >$) and $< G_{01} >$ (ou $< G_{10} >$) of the $SCR \rightarrow ICR$ and $ICR \rightarrow WCR$ phase transition respectively as function of the inverse temperature β for $\chi = -6.0$.

FIG. 6. All the eingenvalues of the Hamiltonian (1) scaled by the number of particles for $\chi = -6.0$ and $N = 6$. They are separated according to the irreducible representation they belong to (see Fig. 7). The quantity n_{max} is the number of eingenstates of each irreducible representation.

FIG. 7. Irreducible representations for $N = 6$.

FIG. 8. Relative contribution of the irreducible representations $P_{[a]}$ for $N = 6$ and $\chi = -6.0$ as function of inverse temperature β.

FIG. 9. Mean field result (solid line) and exact result obtained for $N = 4$ (dot-dashed line), $N = 6$ (dashed line) for the average free energy $\bar{F}$ as function of inverse temperature β for $\chi = -6.0$. The dotted line represents the results for 30 particles, but just considering the symmetric representation. For the SCR, this representation is responsible for the system behavior.

TABLE CAPTIONS

TABLE I. Candidates to minima of free energy found solving equations (17) and (18) for $\theta_3 = 0$ (or π).

Figure 1 (a)

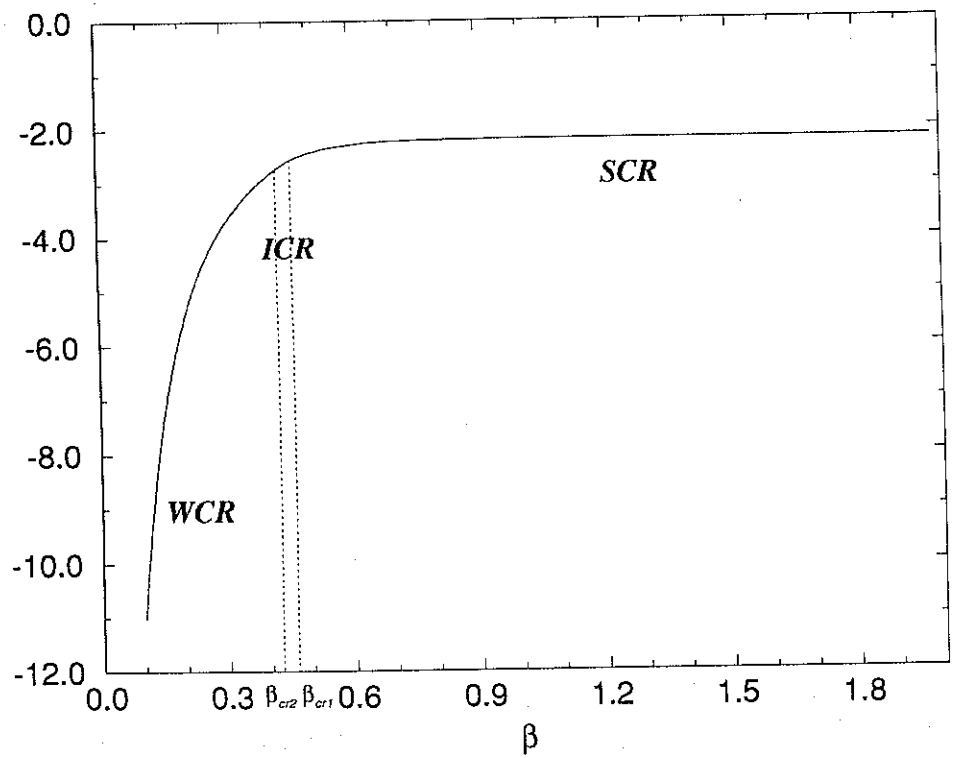

Figure 1 (b)

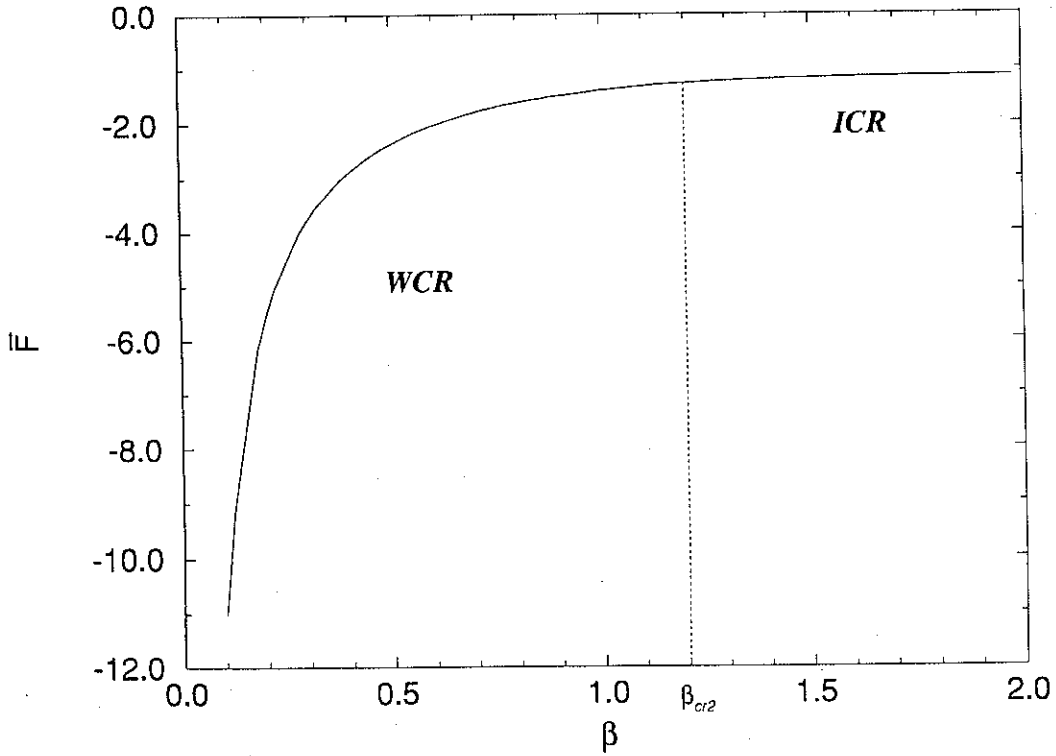

Figure 1 (c)

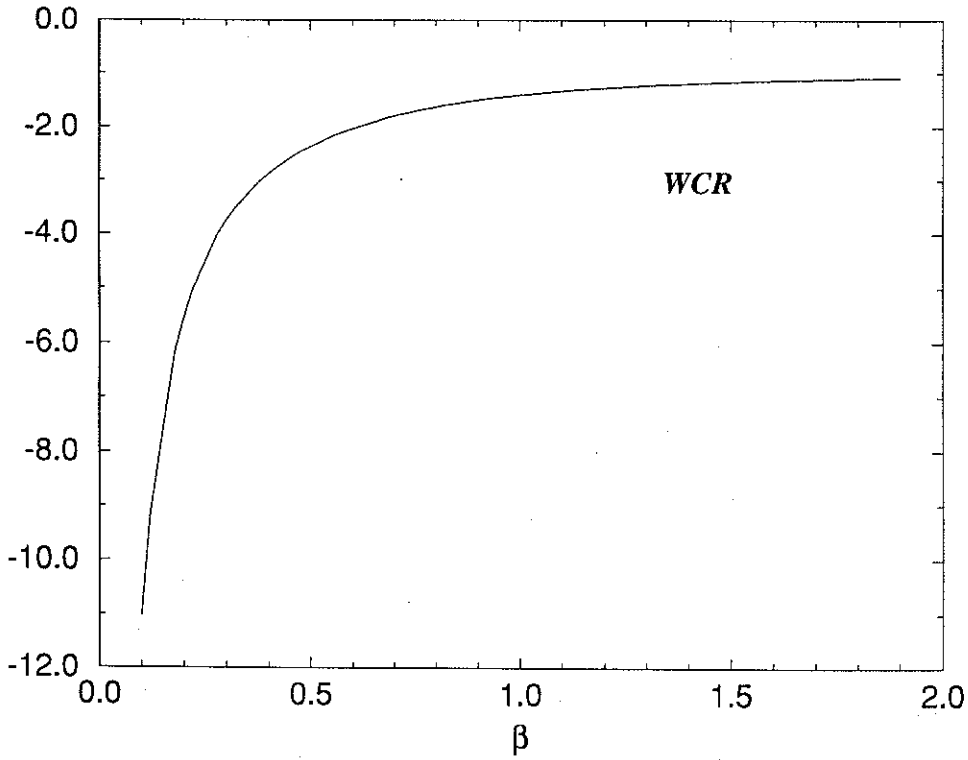

Figure 2 (a)

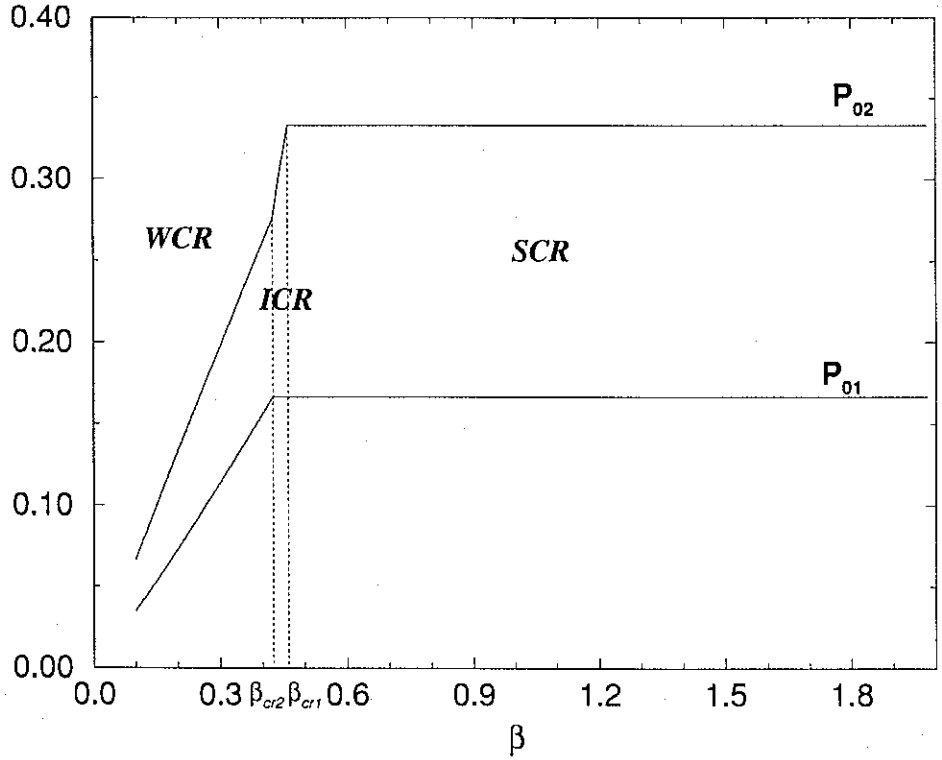

Figure 2 (b)

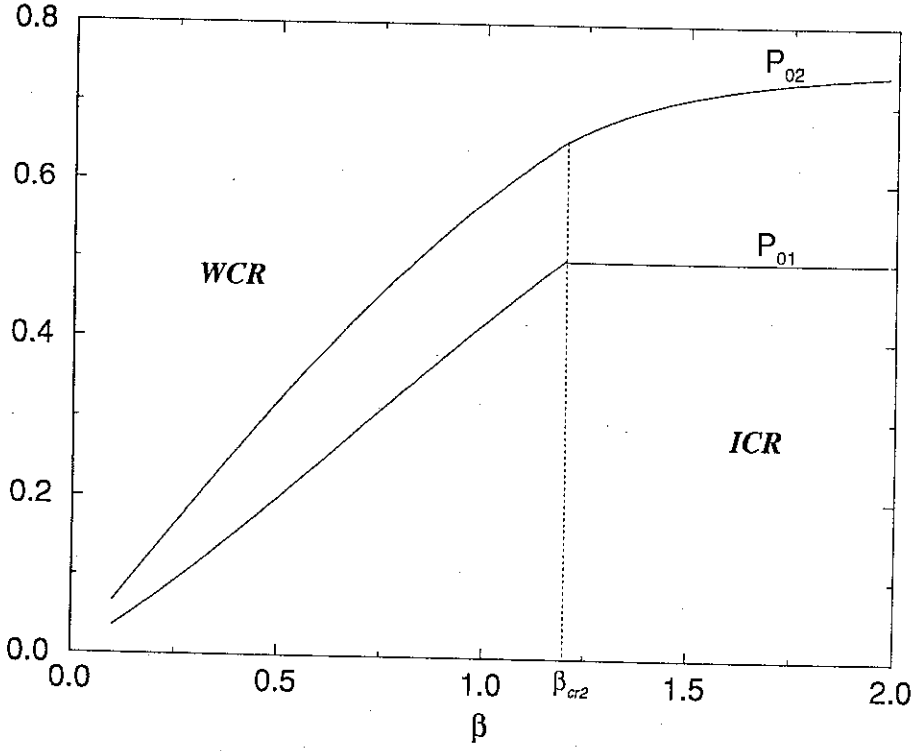

Figure 3

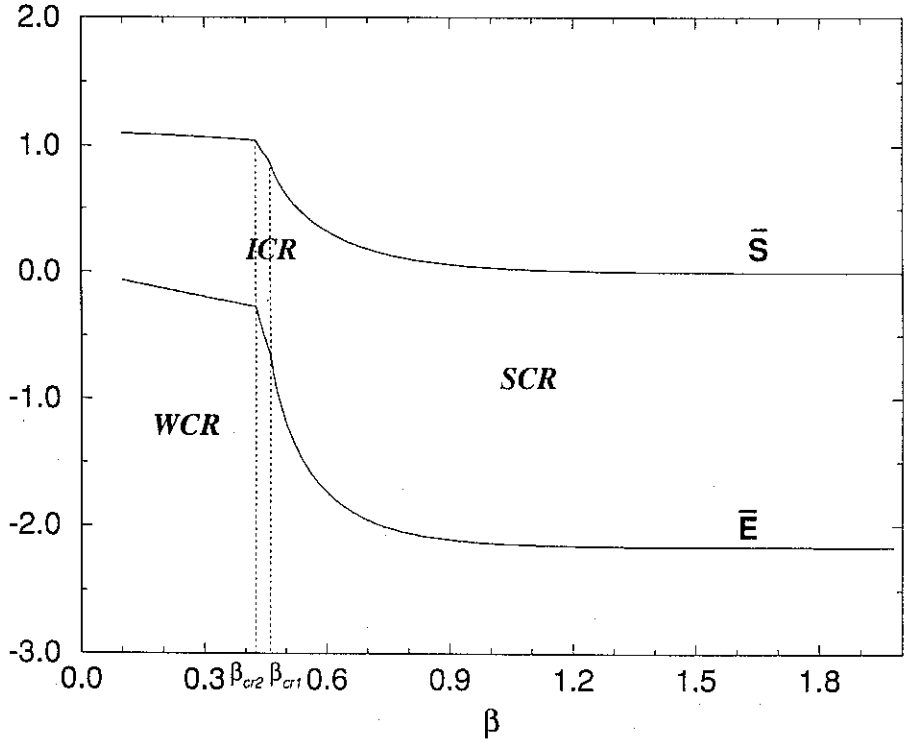

Figure 4

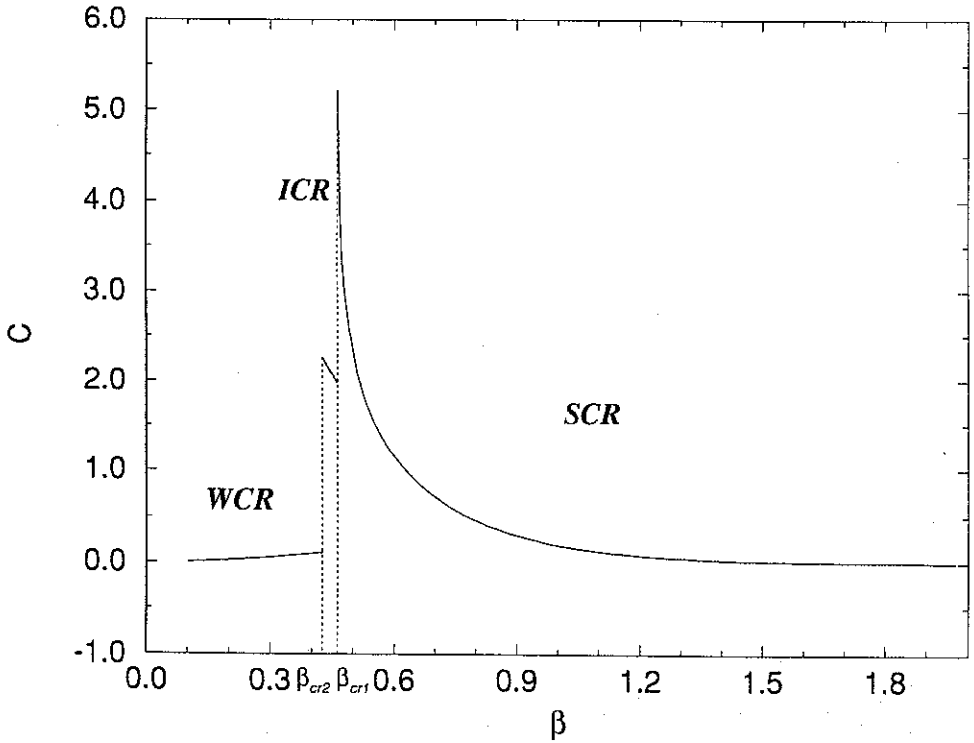

Figure 5

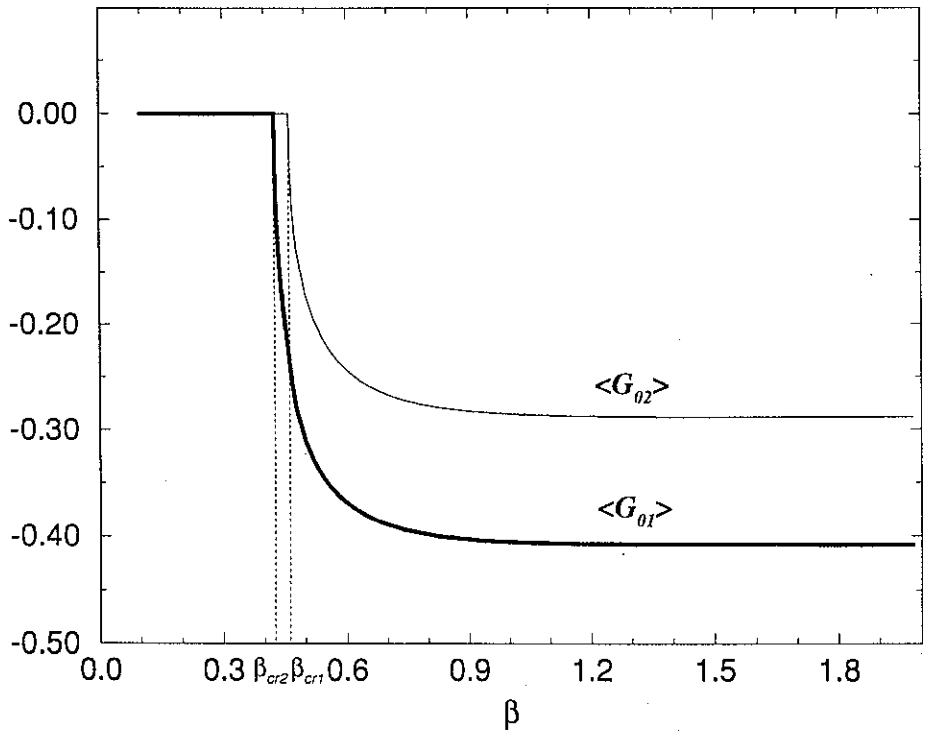

Figure 6

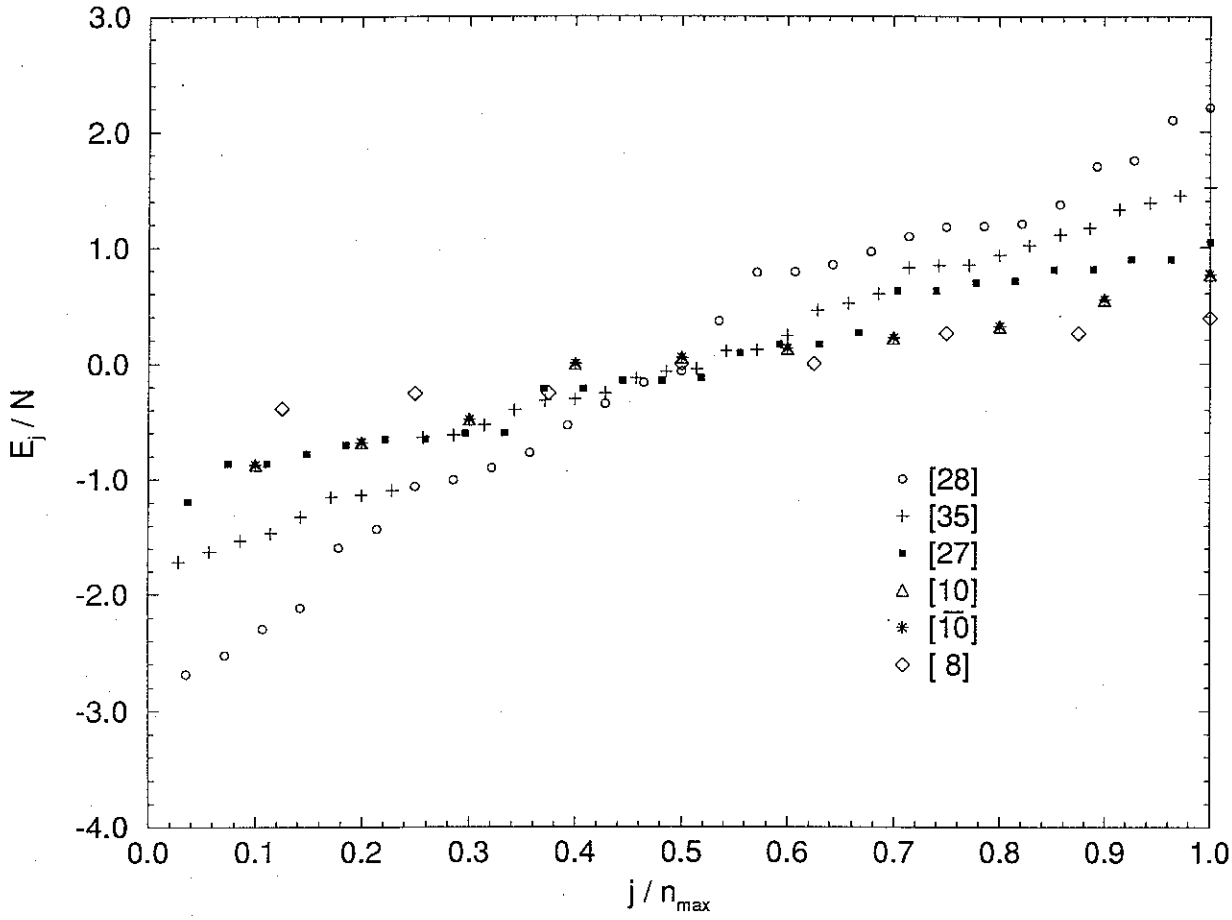

Figure 7

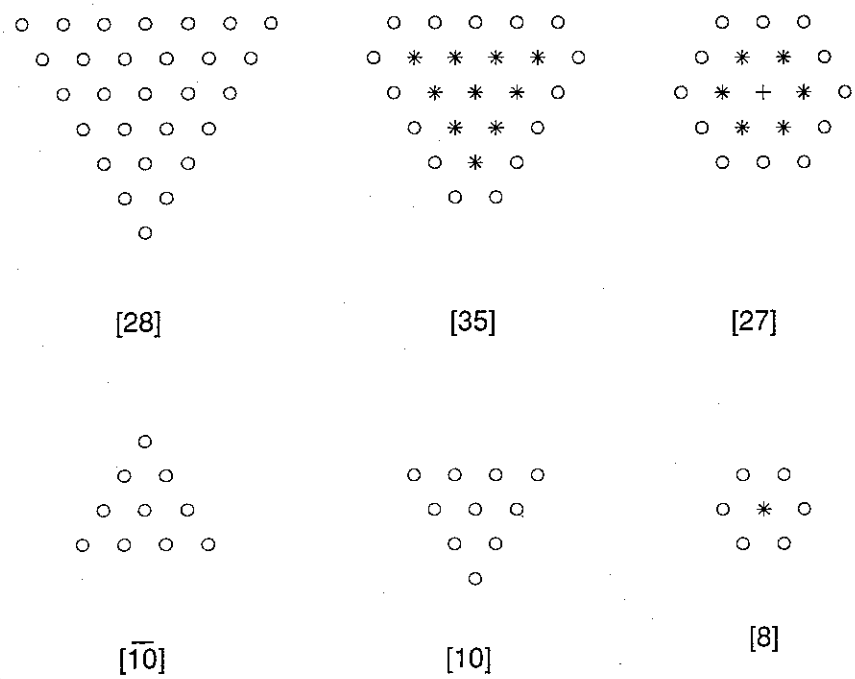

Figure 8

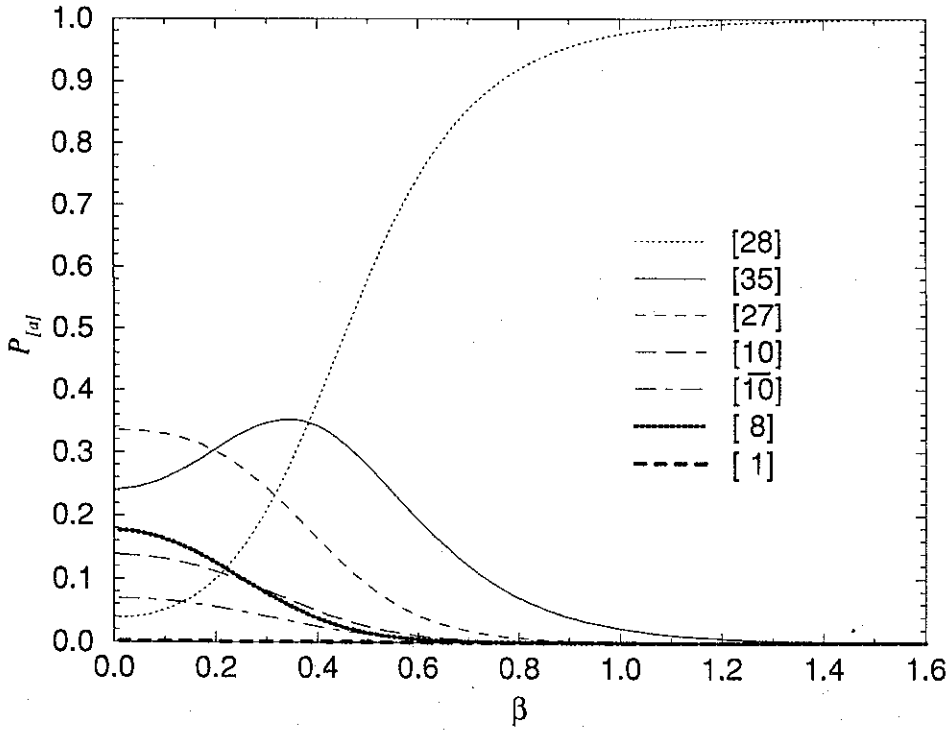

Figure 9

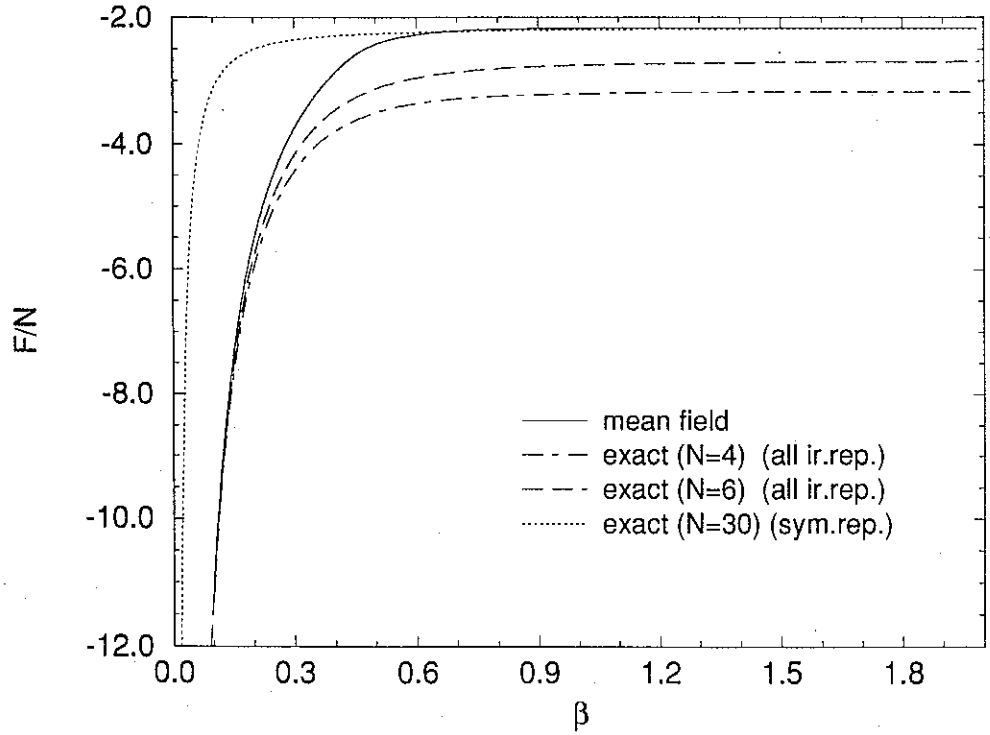

n	θ_1	θ_2	χ range
1	0	0	-
2	0	$\frac{\pi}{2}$	-
3	0	$\frac{1}{2}\arccos\left(\frac{-2}{\chi T_2}\right)$	$\lvert\chi\rvert \geq 2$
4	$\frac{\pi}{2}$	0	-
5	$\frac{\pi}{2}$	$\frac{\pi}{2}$	-
6	$\frac{\pi}{2}$	$\frac{1}{2}\arccos\left(\frac{-1}{\chi T_2}\right)$	$\lvert\chi\rvert \geq 1$
7	-	$\frac{\pi}{2}$	$T_1 = T_2$
8	$\arcsin\sqrt{2+\chi(T_2-2T_1)}$	$\arcsin\sqrt{T_1/T_2}$	$1 \leq \chi \leq 2$
9	$\frac{1}{2}\arccos\left(\frac{-1}{\chi T_1}\right)$	0	$\lvert\chi\rvert \geq 1$
10	$\frac{1}{2}\arccos\left(\frac{1}{\chi(T_2-T_1)}\right)$	$\frac{\pi}{2}$	-
11	$\frac{1}{2}\arccos\left(\frac{3}{3+2\chi(T_2-2T_1)}\right)$	$\arcsin\sqrt{\frac{3+\chi(2T_2-T_1)}{3\chi T_2}}$	$\lvert\chi\rvert \geq 3$

Table I